International Journal of Environment, Agriculture and Biotechnology
Vol-10, Issue-5; Sep-Oct, 2025
Peer-Reviewed International Journal
Journal Home Page Available: https://ijeab.com/
Journal DOI: 10.22161/ijeab

The Study on Soil Erosion and Carbon Sequestration in Zhanjiang City Using RUSLE-InVEST Model

Jinli Zhou, Ruei-Yuan Wang*

School of Sciences, Guangdong University of Petrochem Technology (GDUPT), Maoming 525000, China
*Corresponding author

Received: 21 Aug 2025; Received in revised form: 23 Sep 2025; Accepted: 27 Sep 2025; Available online: 06 Oct 2025

Abstract— *This study aims to reveal the spatiotemporal differentiation characteristics of soil erosion and carbon sequestration in Zhanjiang City and their underlying causes, providing a scientific basis for ecosystem monitoring in the region. Based on the RUSLE-InVEST model and geographic detectors, data from four years (2013, 2017, 2020, and 2023) were selected to analyze the main driving factors and mechanisms of soil erosion, as well as the spatiotemporal variations in carbon sequestration in the study area. The results indicate that soil erosion in Zhanjiang City exhibits significant spatial heterogeneity, with an overall increasing trend in erosion severity. In single-factor analysis, precipitation and land use type factors showed higher explanatory power for soil erosion. In interaction factor analysis, all factor interactions demonstrated either two-factor enhancement or nonlinear enhancement. Overall, the intensity of soil erosion in Zhanjiang City fluctuated over time, and carbon sequestration showed a significant correlation with changes in soil erosion intensity. High-risk erosion areas require prioritized management, and region-specific differentiated governance strategies are recommended based on local conditions.*

Keywords— ***Soil erosion, RUSLE model, InVEST model, Carbon sequestration, Geographic detector***

I. INTRODUCTION

Ecosystems can generate a range of goods and services essential for human well-being, collectively referred to as Ecosystem Services (ES) (Nelson et al., 2009). Since the Millennium Ecosystem Assessment (2005), ecosystem services have become one of the key indicators for measuring ecosystem quality and sustainability. Since then, the assessment of ecosystem services has emerged as a major research topic, with significant progress being made.

Water conservation, soil retention, and carbon sequestration, as key components of ecosystem services, play a crucial role in the synergistic development of ecosystems (Zuo et al., 2024). However, in the context of economic development and urbanization, climate change and land-use alterations are severely impacting global ecosystem services, threatening the sustainable development of human society (Babbar et al., 2021). Consequently, the increase in the greenhouse effect and climate change has become a global concern, particularly as carbon sequestration significantly influences global carbon reduction and mitigates global warming (Deng et al., 2021). Carbon sequestration, as an ecosystem service, may play a vital role in offsetting anthropogenic carbon sources and regulating climate. Moreover, soil erosion severely damages soil resources, affects soil carbon

sequestration, harms ecosystems, and simultaneously hinders crop growth, impeding regional ecological-economic development (Ma et al., 2021). Understanding the impacts and mechanisms of these ecological chains can help address the related scientific issues mentioned above.

Soil erosion is the process by which soil and its parent materials are destroyed, eroded, transported, and deposited under the action of hydraulic forces, gravity, and other factors (Dotterweich, 2013). Soil erosion can lead to a decline in soil quality, deterioration of physical and chemical properties, land desertification, reduced agricultural productivity, sedimentation in rivers and lakes, and many other environmental issues, making it one of the largest global ecological problems (Wang, 2011). Due to China's large population, complex geological conditions, and topographic structures, soil erosion has severely threatened survival and socio-economic development, becoming one of the major challenges for sustainable development in the 21st century (Qi et al., 2011). The multi-scale characteristics of soil erosion and the complexity of its influencing factors impose higher demands on soil erosion prevention and control. Therefore, studying the spatiotemporal distribution characteristics of soil erosion holds special significance and necessity (Yan, 2022).

The Revised Universal Soil Loss Equation (RUSLE) model was developed by the U.S. Department of Agriculture as an improvement upon the Universal Soil Loss Equation (USLE) (Chen, 2011). Due to its straightforward calculation formula and relatively low data requirements, it has become a widely used quantitative estimation model for soil erosion globally (Wu et al., 2012). For example, Hu Xianpei et al. analyzed the spatiotemporal characteristics of soil erosion in Tongren from 1987 to 2015 using the RUSLE model (Hu et al., 2019). Li Yanmeng et al. explored the spatiotemporal evolution patterns of karst soil erosion based on GIS and the RUSLE model (Li et al., 2023). These studies collectively demonstrate that the RUSLE model has a certain applicability in estimating soil erosion in most regions of China (Liang et al., 2019). Additionally, Chen Jinxing et al. (Chen et al., 2016) found that RUSLE is more suitable for areas with significant forest and farmland coverage, while the Chinese Soil Loss Equation (CSLE) is preferable for regions dominated by other land use types. Larger regions are generally more suited for RUSLE (Huang et al., 2025). Given that Zhanjiang covers a relatively large area with substantial forest and farmland coverage, this study adopts the RUSLE model combined with remote sensing and geographic information technology. By extracting factors such as the rainfall erosivity factor (R), soil erodibility factor (K), land use data, cover management factor (C), and support practice factor (P) for Zhanjiang, the study aims to investigate soil erosion in the region.

In addition, regarding the analysis and exploration of carbon sequestration, there is a close relationship between carbon sequestration, soil, and ecological service systems. Soil serves as the largest terrestrial carbon sink for organic carbon. Through organic matter management, soil carbon sequestration can be increased, thereby enhancing its carbon sequestration capacity. This also brings multiple benefits, including improved fertility, soil and water conservation, and environmental protection. Forest management can also increase carbon sequestration by boosting productivity and extending rotation periods, complementing the soil carbon pool to jointly support the health and functionality of ecosystems. In recent years, using the carbon sequestration module of the InVEST model to study the spatiotemporal characteristics of ecosystem carbon sequestration and its relationship with land use patterns has become a hot topic (Wu and Wang, 2023; Zhou, 2025). Compared to other research methods, the InVEST model requires less data and operates faster, enabling spatial mapping of carbon sequestration distribution and dynamic changes. It reflects the relationship between land use changes and carbon sequestration, facilitating the dynamic quantification of ecological service function value (Liu et al., 2021).

Most previous studies have employed single-variable analysis and rarely combined soil erosion with carbon sequestration in research on the same region. Therefore, this study utilizes the RUSLE model for soil erosion analysis, employs geographic detectors to examine its driving factors, and explores the spatiotemporal characteristics of ecosystem carbon sequestration using the carbon module of the InVEST model. By adopting a

coupled approach, it aims to provide an in-depth understanding of the ecological service system in the study area, thereby offering a scientific reference.

II. STUDY AREA AND DATA SOURCES

2.1 Study Area

Zhanjiang City (20°13′N-21°57′N, 109°31′E-110°58′E) is located in the southwest of Guangdong Province. It serves as the central city of the western Guangdong and Beibu Gulf urban agglomeration and is one of China's first batch of coastal open cities (Figure 1). The total area under its jurisdiction is 13,263 km², with a coastline stretching 2,023.6 km, including 1,243.7 km of mainland coastline and 779.9 km of island coastline. Situated south of the Tropic of Cancer, it enjoys a tropical northern marginal monsoon climate, with an average annual temperature ranging between 23°C and 24°C. The region experiences distinct monsoons, diverse climate types, abundant heat, plentiful rainfall, and clearly defined wet and dry seasons. Frequent and severe meteorological disasters such as typhoons and torrential rain-induced floods make the area prone to soil erosion.

Zhanjiang is located in the southern red soil region of China, characterized by uneven spatial and temporal distribution of precipitation, acidic, barren, and heavy-textured soil properties. Predominantly composed of red soil, which is relatively heavy and not prone to forming granular structures, these soil characteristics are prone to causing soil erosion. Coupled with unreasonable land development and utilization, it is highly susceptible to ecological and environmental issues such as soil desertification, salinization, water and soil loss, and soil pollution.

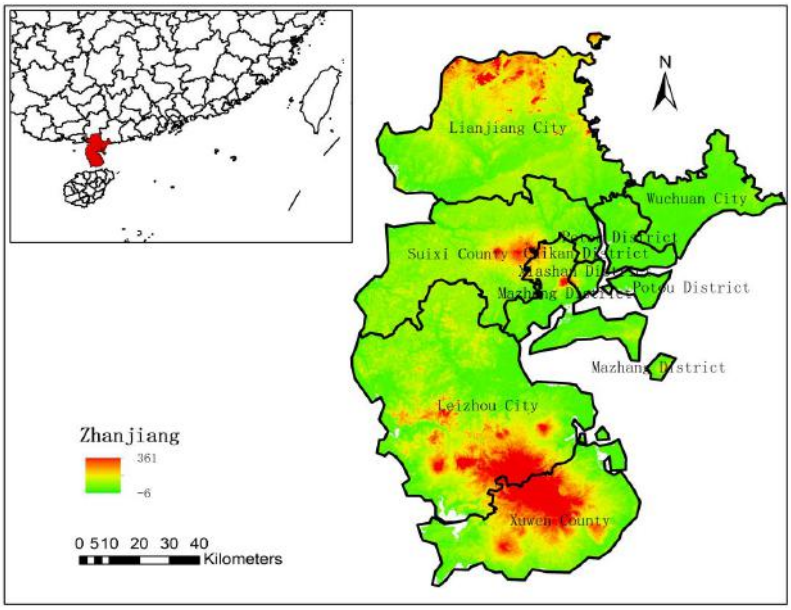

Fig.1 Geographical Location and Elevation Distribution Map of Zhanjiang City

2.2 Data Sources

The elevation data with a spatial resolution of 30 m was obtained from the Geospatial Data Cloud (http://www.gscloud.cn) for creating terrain generalization maps and LS factors; Landsat 8 data was downloaded and processed in ENVI to derive NDVI (Normalized Difference Vegetation Index), which was then used to calculate FVC (Fractional Vegetation Cover) through confidence extraction and formula computation, ultimately applied to determine the vegetation cover factor.

The world soil database (HWSD) was downloaded from the National Earth System Science Data Center (https://www.geodata.cn), and after mask extraction and raster calculation, the K factor (soil erodibility factor) was obtained. Rainfall data for the study area was also acquired, and the R (Rainfall) factor was calculated using ArcGIS raster computation.

Land use/land cover data was downloaded from the Resource and Environment Science Data Center (http://www.resdc.cn). Additionally, GDP (Gross Domestic

Product) data was sourced from the Resource and Environment Science Data Registration and Publishing System (http://www.resdc.cn/DOI, 2017. DOI: 10.12078/2017121102), while population density data was retrieved from the Zenodo database (https://zenodo.org/records/11179644) for investigating the influencing factors of soil erosion using geographic detectors. The data required for model operation and their sources are listed in Table 1.

Table 1 Description of Research Data Sources and Uses

Data category	Data source	Purpose
Annual precipitation	Downloaded from the National Earth System Science Data Center (https://www.geodata.cn),	Generate R-factor layer
HWSD (Harmonized World Soil Database)		Generate K-factor layer
30m DEM	Geospatial Data Cloud（http：//www.gscloud.cn）	Calculate LS factor
NDVI		Generate C-factor layer
Global Land Use/Land Cover Map（LUCC）	Resource and Environmental Science Data Center (https://www.resdc.cn/)	Generate land use layers
GDP data	Resource and Environmental Science Data Registration and Publishing System（http：//www. resdc.cn/DOI）	Geographic Detector Parameters
Population density data	Zenodo Database （https：//zenodo.org/records/11179 644）,	Geographic Detector Parameters

III. METHODOLOGY

This study employs the RUSLE model to assess soil erosion, utilizes a geographic detector to analyze its driving factors, and investigates the spatiotemporal variations in ecosystem carbon sequestration using the carbon module of the InVEST model. The RUSLE model incorporates data such as annual precipitation, HWSD, NDVI, and DEM for analysis, while the InVEST model primarily relies on the Global Land Use/Land Cover Map (LUCC) as its analytical material. The geographic detector analysis involves 11 factors, encompassing both natural and anthropogenic elements. Finally, the analytical results are integrated to derive scientific conclusions for the study area (Figure 2).

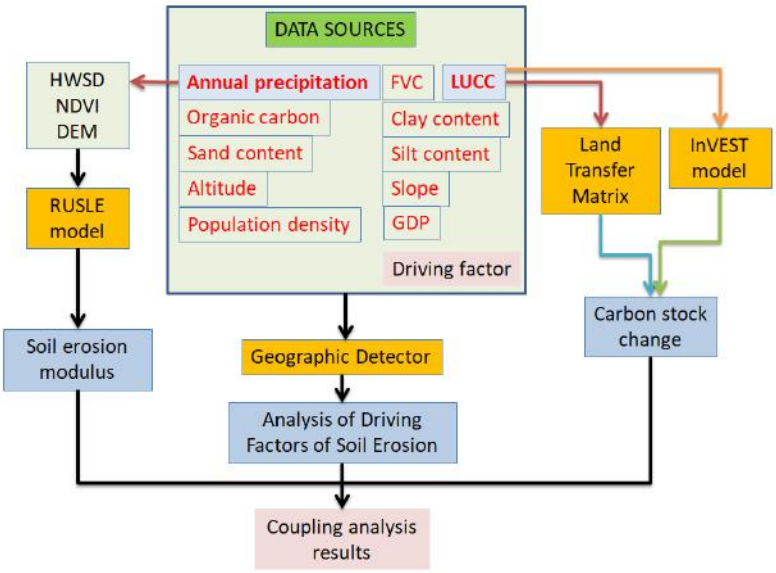

Fig.2 Technical Framework of This Study

3.1 Soil Erosion Model Parameter Construction

This study employs the RUSLE model, which features standardized and clear definitions for each factor, along with a straightforward calculation process. The calculation formula is as follows:

$$A=R\times K\times LS\times C\times P \quad (1)$$

In the formula: A is the soil erosion modulus, Unit: t/(hm^2·a); R is the rainfall erosivity factor, in MJ· mm/(hm^2·h·a); K is the soil erodibility factor, in t·h/(MJ·mm); LS is the slope length and steepness factor, dimensionless; C is the cover and management factor, dimensionless, ranging from 0 to 1.

3.1.1 R Factor

Precipitation is one of the important causes of soil erosion, mainly triggered by the kinetic energy carried by raindrops impacting soil particles and causing erosion. The R value is a function of rainfall energy and intensity, generally used to reflect the impact of rainfall on soil erosion (Wang et al., 2005). This study adopts the "Guidelines for Calculating Soil Loss in Production and Construction Projects SL773-2018." After obtaining annual precipitation data from 2012 to 2022, the precipitation erosivity factor was calculated using Formula (2).

$$R=0.067P_d^{1.627} \quad (2)$$

In Equation (2), R represents the multi-year average rainfall erosivity factor, with units of MJ·mm/(hm²·h); Pd denotes the multi-year average rainfall, measured in mm, and the spatial distribution of the precipitation erosivity factor is calculated accordingly.

3.1.2 K Factor

Soil erodibility refers to the spatial variation in the ability of soil's inherent physicochemical structure to resist erosion at different locations, serving as a crucial quantitative parameter for assessing soil sensitivity to erosion. This study employs the widely used calculation methods from the Erosion Productivity Impact Calculator (EPIC) model proposed by Sharpley et al. (1990) and Williams et al. (1983). Additionally, based on the modified algorithm for soil erodibility factor (K) in Chinese regions introduced by Zhang et al. (2007), the soil erodibility factor (K) for the study area was calculated using the following formula:

$$SN = 1 - SAN/100 \quad (3)$$

$$K_{epic}=\left\{0.2+0.3\exp\left[-0.0256SAN\left(1-\frac{SIL}{100}\right)\right]\right\}\times\left(\frac{SIL}{CLA+SIL}\right)^{0.3}\times\left[1-\frac{0.25C}{C+\exp(3.72-2.95C)}\right]\times\left[1-\frac{0.7SN}{SN+\exp(-5.51+22.9SN)}\right] \quad (4)$$

$$K=-0.01383+0.51575\times Kepic \quad (5)$$

3.1.3 L、S Factor

Slope length and gradient are fundamental topographic factors. Slope length refers to the distance from the starting point of surface runoff generation on a slope to the point where runoff converges into a gully (Wang et al., 2020). A longer slope length indicates greater runoff accumulation and stronger erosive power. Gradient refers to the degree of inclination at a specific point on the land surface. By influencing the velocity of water flow, gradient affects infiltration rate, runoff volume, and soil scouring, making it the best micro-scale indicator for soil erosion assessment (Wang et al., 2020). The LS factor effectively reflects the influence of topography on rainfall erosion. In this study, DEM was used to extract the LS factor.

$$L=\left(\frac{\lambda}{22.13}\right)^m \quad (6)$$

$$\lambda=l\times\cos a \quad (7)$$

In the formula: L is the slope length factor (dimensionless); λ is the horizontal projection slope length (m), which is the length of surface water flow along the direction; α is the slope value of the water flow area; m is the variable slope exponent (Jin, 2019).

When θ < 0.57°, m = 0.2.

When 0.57° ≤ θ < 1.72°, m = 0.3.

When 1.72° ≤ θ < 2.86°, m = 0.4.

When 2.56° ≤ θ, m = 0.5.

The slope calculation is based on grading. For slopes below 10°, the McCoolDK formula (McCool et al., 1987) is used, while for slopes above 10°, the formula calibrated by Liu (2001) is applied:

$$S=\begin{cases}10.80\times\sin\theta+0.03 & \theta<5^\circ\\ 16.80\times\sin\theta-0.50 & 5^\circ<\theta\le10^\circ\end{cases} \quad (8)$$

$21.91\times\mathrm{Sin}\theta-0.96 \quad \theta>10°$

Where: S is the slope factor (dimensionless); θ is the slope (°)

3.1.4 C Factor

Vegetation coverage (C) refers to the percentage of vegetation in the vertical projection area relative to the total area. In this study, the pixel dichotomy model was used to calculate the vegetation coverage of the study area as a measure of vegetation factors, with the calculation formula as follows:

$$Fg=(NDVI-NDVI_{soil})/(NDVI_{veg}-NDVI_{soil}) \quad (9)$$

In the equation, Fg represents vegetation coverage, NDVIsoil is the NDVI value of pure soil pixels, which corresponds to the NDVI value closest to the 0.5% position in the minimum NDVI probability distribution table; NDVIveg is the NDVI value of pure vegetation pixels, corresponding to the NDVI value closest to the 0.5% position in the maximum NDVI probability distribution table. By downloading Landsat8 OIL_TIRS product data and performing radiometric calibration, atmospheric correction, and NDVI calculation, the vegetation coverage of Zhanjiang City in 2016 was estimated.

3.1.5 P Factor

The P-value of the soil conservation factor refers to the ratio of soil erosion on sloping farmland with conservation measures to that without such measures under otherwise identical conditions, reflecting the efficacy of these measures in reducing soil erosion. The value ranges from 0 to 1, with P=1 indicating no soil conservation measures are implemented. Based on previous research (Zheng et al., 2023), the assigned values are as follows: Cropland is assigned 1, forestland 0.3, grassland 0.6, impervious surfaces 0.2, water bodies 0.7, and bare land 0.8.

3.2 Soil Erosion Characterization Index

3.2.1 Comprehensive Index Assessment of Soil Erosion

To compare and analyze soil erosion conditions across different units, a comprehensive soil erosion index (Yang et al., 2000) can be used. The grading values for hydraulic erosion—slight, mild, moderate, strong, extremely strong, and severe—are assigned as 0, 2, 4, 6, 8, and 10, respectively.

3.2.2 Soil Erosion Intensity Dynamic Degree

The dynamic degree of soil erosion intensity is an indicator that depicts the rate and magnitude of regional differences in a certain soil erosion intensity over a period, aiming to reflect the severity and overall trend of its changes (He et al., 2024). When J is positive, it means that the area of a certain soil erosion intensity has increased during the study period, indicating an intensification of soil erosion at that intensity; when J is negative, it indicates a mitigation of soil erosion at that intensity. The calculation formula is as follows:

$$J=\frac{U_b-U_a}{U_a}\times\frac{1}{T}\times 100\% \quad (10)$$

In the formula: J represents the dynamic degree of soil erosion at a certain intensity; Ua and Ub are the areas of a certain erosion intensity at the beginning and end of the study period, respectively; T is the duration of the study period.

3.2.3 Entropy of Soil Erosion Intensity

The lower the information entropy of soil erosion intensity, the greater the proportion of slight erosion, and the smaller the proportion of other intensities of soil erosion, indicating an improvement in soil erosion conditions. The calculation formula is as follows:

$$H=-\sum_{I=-1}^{n} Q_i\times \ln Q_i \quad (11)$$

In the formula: H represents the information entropy of soil erosion intensity; Qi is the proportion of the area of soil erosion at the i-th intensity level to the total area of soil erosion in the watershed; n is the number of soil erosion intensity levels (Huang et al., 2025).

3.3 Geographical Detector

Based on the geographic detector, by combining different spatial data discretization methods with discontinuous parameters, the q value is used to quantitatively measure the quality of the discretization parameters. The larger the q value, the stronger the explanatory power of X on Y. The calculation formula is as follows:

$$q=1-\sum_{h=1}^{L} N_h\times\sigma^2{}_h/N\sigma^2 \quad (12)$$

In the formula: q is the detection value of the driving factor; it refers to the explanatory power of the independent variable X on the dependent variable Y, with a range of [0, 1]. The larger the value, the stronger the explanatory power of X on the spatial differentiation of Y. N is the total number of samples; L is the number of strata for variable X or Y; h is the number of strata for variable X

or Y; N_h is the number of samples in the h-th stratum; σ^2 is the total variance of the dependent variable Y for the entire population; σ^2 is the variance of Y values in the h-th stratum.

This study established random sampling points for fishing net extraction within Zhanjiang City, extracting various classification values to their corresponding sample points. Based on the GD package in R language, equal interval, natural breaks, and quantile methods were selected as discretization approaches, with classification numbers ranging from 3 to 7 categories. Subsequently, the geographical detector was employed to analyze the influence of various factors in the RUSLE model on soil erosion. Using the factor detector and interaction detector modules within the model, the explanatory power of 11 influencing factors (land use type, annual rainfall, vegetation coverage, elevation, slope, sand content, silt content, clay content, organic carbon content, GDP, and population density) on the spatial heterogeneity of soil erosion was quantified.

3.4 Carbon Sequestration Estimation

Carbon sequestration services, as a core regulatory function in addressing climate change, directly influence atmospheric carbon cycles and global climate patterns through ecosystem carbon sequestration and storage processes. They serve as a vital natural solution for achieving the "dual carbon" goals, with their quantitative research providing a scientific basis for carbon sink accounting and climate policy formulation (Zhou, 2025). This study utilizes the Carbon module within the InVEST model to estimate total carbon sequestration based on the sum of carbon pools corresponding to land use types, calculated using the formula (13):

$$Ci\_tot = Ci\_above + Ci\_below + Ci\_soil + Ci\_dead \quad (13)$$

i represents the ith land use type; Ci_tot denotes the total carbon sequestration, Ci_above represents the aboveground biomass carbon sequestration, Ci_below indicates the underground biomass carbon sequestration, Ci_soil stands for the soil carbon sequestration, and Ci_dead refers to the dead organic matter carbon sequestration. The units of the aforementioned carbon sequestration are all in tons. Based on previous studies, the carbon density values c for various land use types in Guangdong Province were compiled, as shown in Table 2 (Dai et al., 2025).

Table 2 Carbon Density c (/t/hm2) of Land Use Types in Guangdong Province

Land use type	ci_above	ci_below	ci_soil	ci_dead
Cropland	15.74	3.15	10.84	0.00
Forestland	19.24	5.77	19.28	2.82
Grassland	16.06	83.50	9.99	0.24
Water bodies	0.28	1.37	3.03	1.24
Construction Land	11.29	2.26	17.97	0.00
Bare land	13.92	2.78	5.33	0.00

IV. RESULTS AND ANALYSIS

4.1 Spatiotemporal Analysis of Soil Erosion Models

Zhanjiang is in the southern red soil hilly region within the water erosion zone, classified under the southern red soil hilly area. According to the "Classification and Grading Standards for Soil Erosion" (SL190 - 2007), its permissible soil erosion modulus (allowable soil loss) is 500 t/（km²·a）, equivalent to 5 t/（hm²·a）. Analysis reveals that the average erosion modulus in Zhanjiang City is 138.7 t/（hm²·a）, exceeding the permissible soil erosion modulus for the study area. Additionally, the analysis indicates that the average soil erosion volume in Zhanjiang City reaches 1.3064 million tons.

Analysis of various factors in the erosion model reveals that the R-factor exhibits fluctuating changes, with an overall "first decline then rise" trend from 2013 to 2023 (reaching its lowest point in 2020). Significant peaks occurred in 2013 and 2017, largely aligning with changes in soil erosion modulus, making it the core driving factor of erosion (Figure 3a). The C and P factors remained relatively stable. The C-factor (vegetation factor) mostly maintained within the range of 0.8-1.0 across most districts and counties over the long term, with only minor

fluctuations in a few years/regions (Figure 3b).

The P-factor (soil and water conservation measures factor) also remained relatively stable, though some districts and counties (e.g., Chikan District and Mazhang District) showed a slow decline from 2013 to 2023 (Figure 3c). Over time, the soil erosion modulus (K-factor) in most districts and counties displayed a "first decrease then increase" trend (Figure 3d): from 2013 to 2020, the modulus decreased in sync with the decline in the R-factor, while from 2020 to 2023, it rose again as the R-factor rebounded. Regional differences were significant: agricultural districts and counties such as Leizhou City and Suixi County, influenced by both natural and human factors, had high erosion modulus values strongly linked to the R-factor. In contrast, areas like Chikan District and Mazhang District, characterized by gentle terrain and enhanced conservation measures, exhibited lower modulus values with suppressed growth, confirming the buffering effect of vegetation and measures on erosion.

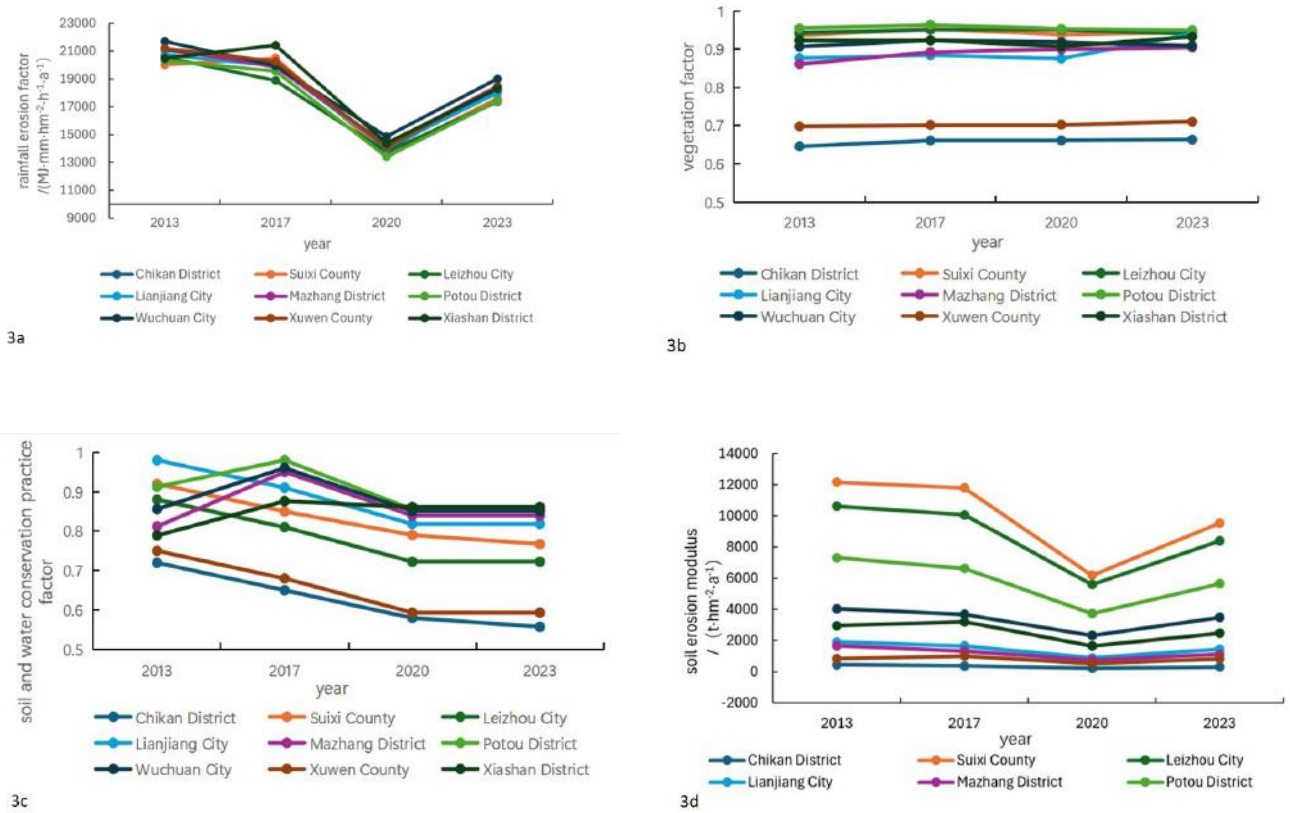

Fig.3. Factor Variation and Soil Erosion Modules from 2013 to 2023

4.2 Comprehensive Assessment of Soil Erosion Levels

This study refers to the "Classification and Grading Standards for Soil Erosion" (SL190-2007) issued by the Ministry of Water Resources of the People's Republic of China, dividing soil erosion intensity into six levels: slight, mild, moderate, strong, extremely strong, and severe erosion. Areas with mild erosion and above are considered as regions affected by soil erosion.

As shown in Figure 4, the overall trend of soil erosion in Zhanjiang City is dominated by slight erosion, accounting for approximately 98.13% of the total erosion area. From 2013 to 2023, the area of slight erosion exhibited a trend of first decreasing and then increasing, with an average rate of 0.061 km²/year. The area of mild erosion showed a similar trend of first decreasing and then rising, with an average rate of -0.064 km²/year. Meanwhile, the areas of moderate, strong, extremely strong erosion all displayed a pattern of initial decline followed by an increase, with average rates of 0.053 km²/year, 0.033 km²/year, and 0.001 km²/year, respectively.

In terms of spatial distribution, Leizhou City had the highest proportion of slight erosion area, followed by

Lianjiang City, while Wuchuan City had the lowest proportion. Additionally, in 2020, the proportion of slight erosion area experienced a slight decline, while the proportions of other erosion categories increased, indicating a worsening trend of erosion in some regions.

As shown in Figure 5, soil erosion in the study area peaked in 2020, reaching 927,500 tons. The erosion intensity in Xiashan District was relatively low, indicating better ecological conditions and more stable vegetation coverage in the area. In contrast, Leizhou City experienced higher erosion levels, reflecting poorer ecological conditions, lower vegetation coverage, and weaker soil and water conservation measures. According to Figure 6, slight erosion was the dominant intensity level in the study area. Overall, the distribution of erosion intensity grades showed a pattern of lower levels in the northwest and higher levels in the southeast. The northern regions had relatively lower soil erosion modulus, while the eastern and southern regions exhibited higher values. In Leizhou City, located in the south, the areas affected by slight and moderate erosion increased significantly.

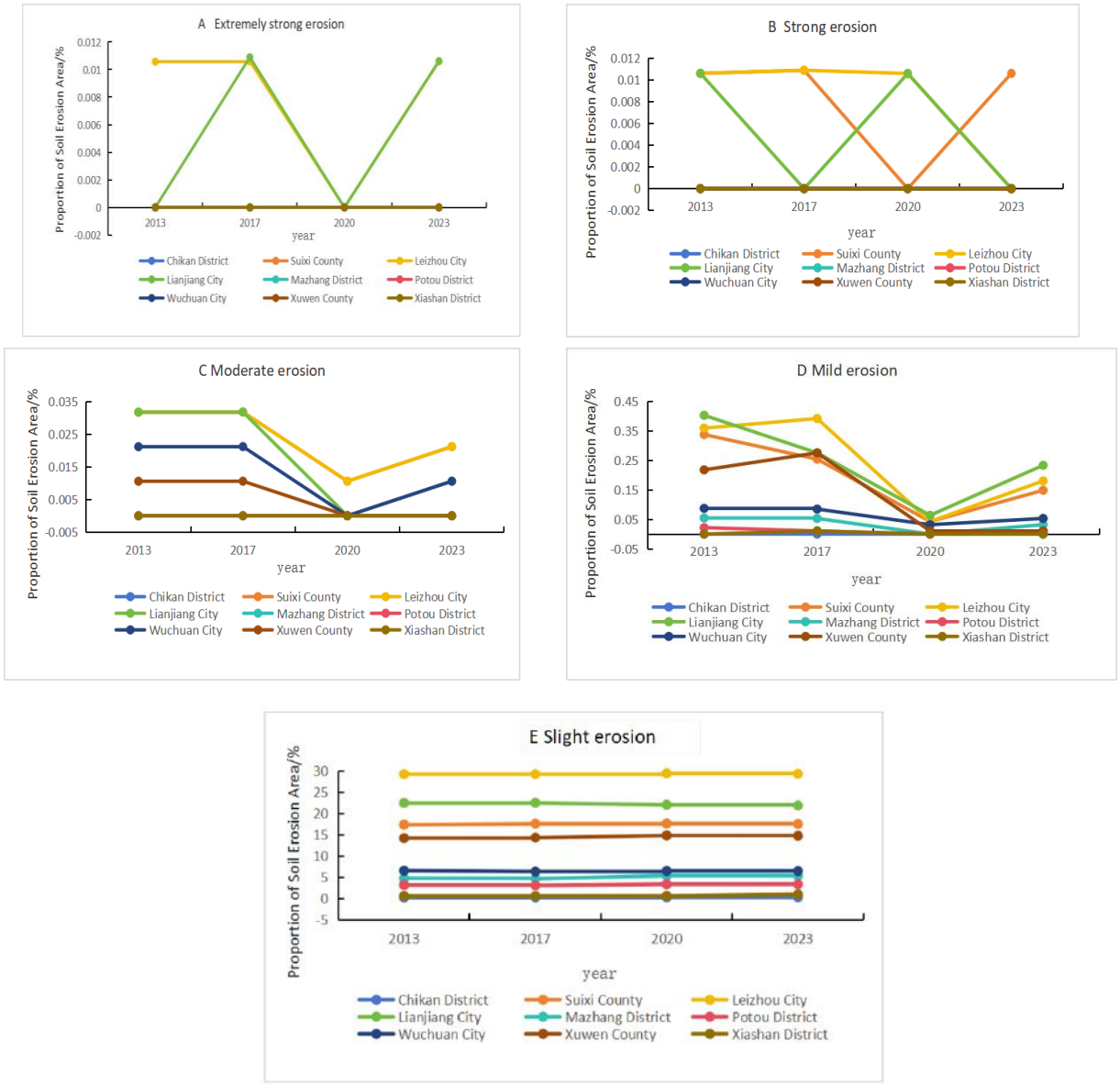

Fig.4 Proportion of Soil Erosion Area

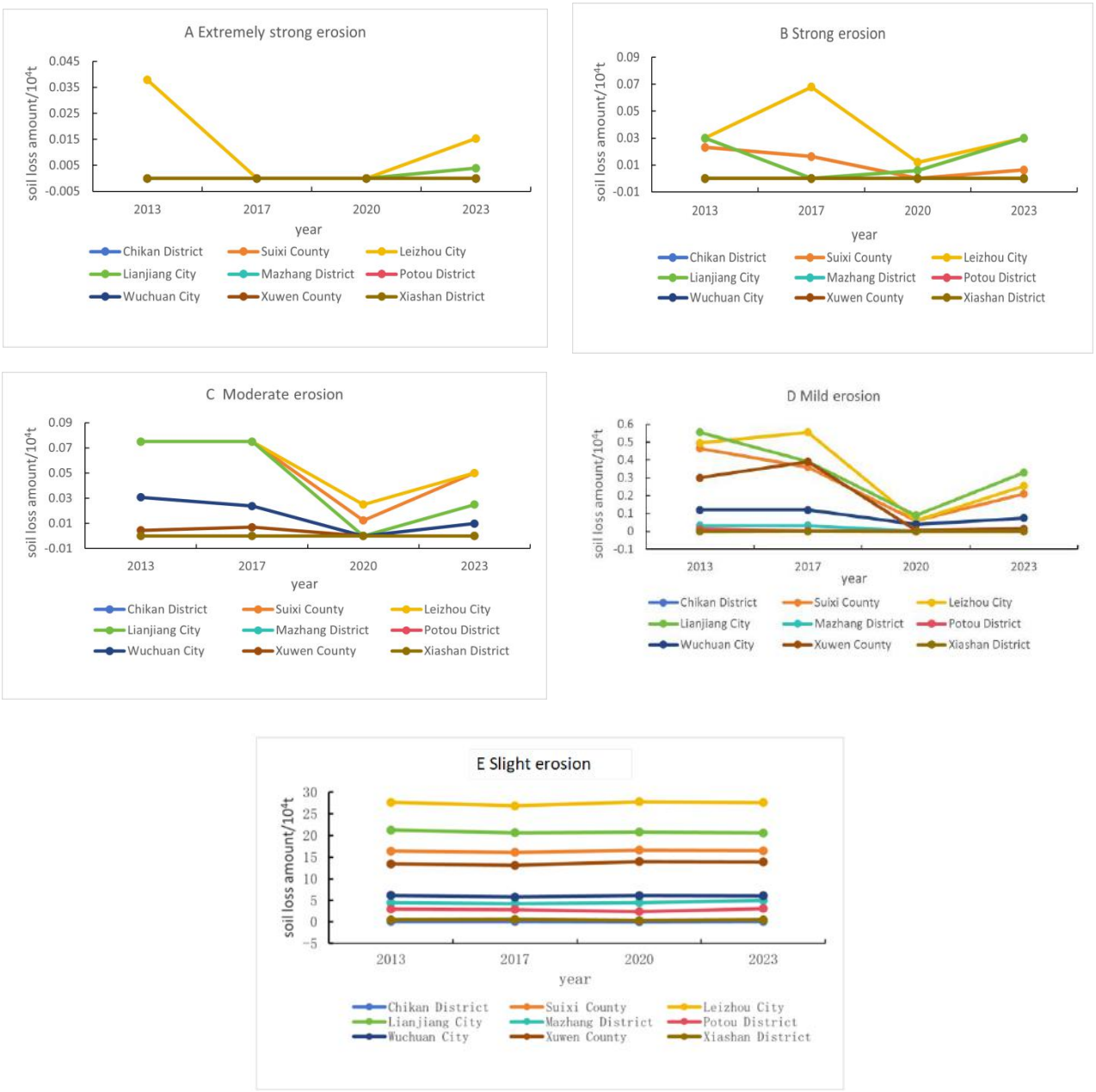

Fig.5 Spatiotemporal Statistics of Soil Erosion

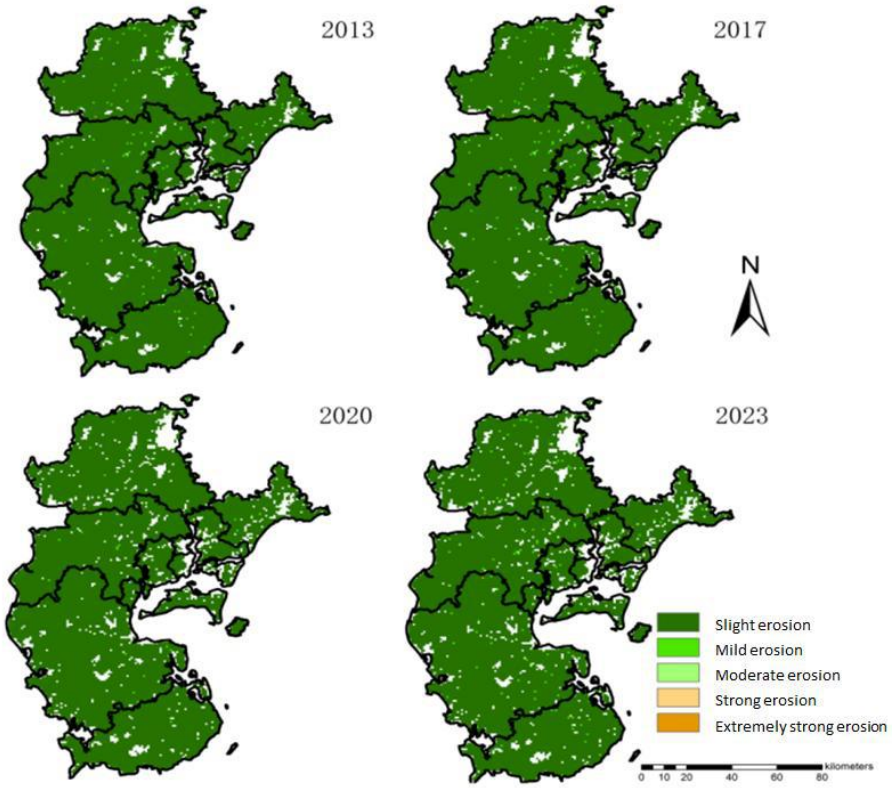

Fig.6 Distribution Map of Soil Erosion Intensity from 2013 to 2023

4.3 Dynamic Changes in Soil Erosion Levels

From 2013 to 2023, the trend of area transfer changes in different erosion intensity levels in the study area was not significant (Figure 7). During the periods 2013–2017, 2017–2020, and 2020–2023, 96.44%, 88.70%, and 99.16% of the areas, respectively, showed no change in erosion intensity levels. Over the study period, the newly added and transferred areas of slight erosion were 3.51 km² and 1.49 km², accounting for 3.70% and 1.57% of the total area, respectively. The reduced and transferred area of mild erosion was 0.61 km², accounting for 0.63% of the total area. Moderate and strong erosion trends decreased by 0.059% and 0.0073%, respectively, indicating minimal changes in soil erosion intensity in the study area.

As shown in Figure 8, the dynamic degree of slight erosion was predominantly negative from 2013–2017 and 2020–2023, indicating a gradual reduction around such regions, with more areas transitioning to mild erosion and higher grades. Meanwhile, the dynamic degrees of mild, moderate, strong, and extremely strong erosion were mainly positive, suggesting an increasing area of erosion and a worsening trend in erosion conditions. Particularly during 2020–2023, the dynamic degree of strong erosion reached its peak at 412.5%. Although the dynamic degrees of most erosion intensities were negative during 2017–2020, indicating some mitigation of erosion, the dynamic degrees of moderate and strong erosion rose again to 131.8%, 63.40%, and 412.5% in 2020–2023, demonstrating that the trend of intensifying erosion has not been effectively curbed.

Comparing the comprehensive soil erosion index with the changes in information entropy of soil erosion intensity in the study area (Table 3), the trends show similar patterns. Between 2013 and 2017, the comprehensive index and information entropy values were comparable, indicating that the overall intensity of soil erosion in the study area did not change significantly. From 2017 to 2020, the comprehensive index showed a slight decline, reaching 0.010 in 2020, while the information entropy also decreased from 0.091 in 2017 to 0.027 in 2020. This suggests that during this period, the extent of soil erosion narrowed, and the intensity of erosion weakened.

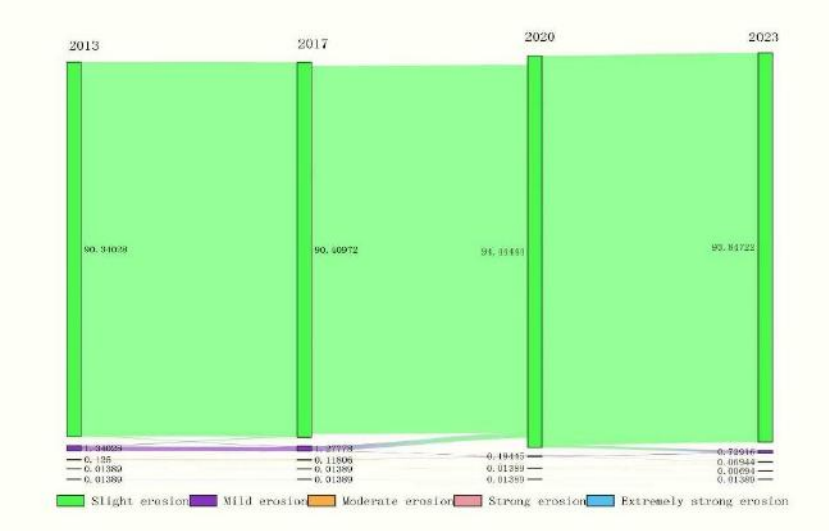

Note A: Slight erosion B: Mild erosion C: Moderate erosion D: Strong erosion E: Extremely strong erosion

Fig.7 Soil Erosion Intensity Grade Transfer Map

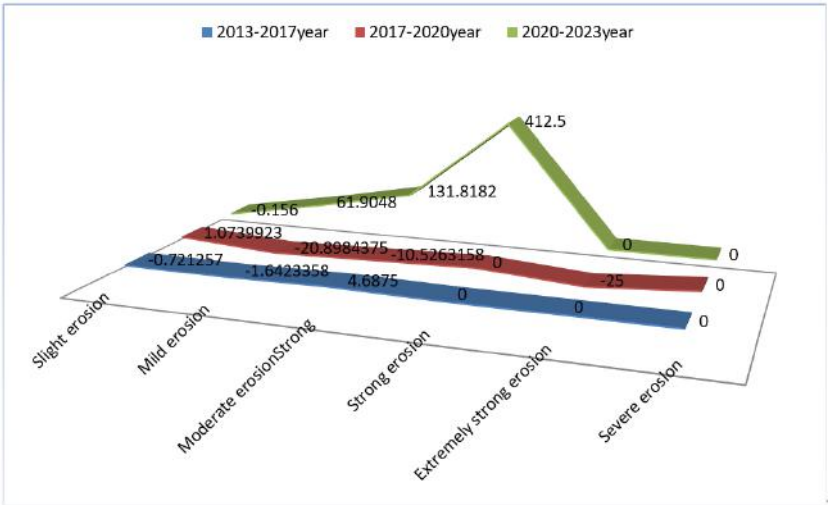

Fig.8 Dynamic Degree of Soil Erosion Intensity

Table 3 Soil Erosion Characterization Indexes in Zhanjiang City

Year		2013Year	2017Year	2020Year	2023 Year
Characterization Index	Composite Index	0.0378	0.038	0.010	0.0678
	Information entropy	0.0911	0.091	0.027	0.114

4.4 Analysis of Factors Influencing Soil Erosion

The significance analysis of soil erosion influencing factors (Table 4) reveals that the order of factors affecting the soil erosion modulus from greatest to least is annual precipitation (q=0.4648) > land use type (q=0.2855) > organic carbon content (q=0.1959) > slope (q=0.1922) > sand content (q=0.1917) > elevation (q=0.1879) > GDP (q=0.1506) > clay content (q=0.1453) > silt content (q=0.1304) > population density (q=0.1281) > vegetation coverage (q=0.1281). The results indicate that the primary factors contributing to the spatial variation of soil erosion modulus are natural environmental factors, with annual precipitation having the highest explanatory power, followed by land use type and organic carbon content.

Among anthropogenic factors, GDP exhibits the greatest explanatory influence.

Table 4 q-values of Driving Factors

Category	Factors	q value	p value
Natural Factors	LUCC	0.2855	0.2340
	Annual precipitation	0.4648	0.0080
	FVC	0.1281	0.7911
	Organic carbon content	0.1959	0.5168
	Clay content	0.1453	0.2406
	Sand content	0.1917	0.5275
	Silt content	0.1304	0.7131
	Altitude	0.1879	0.5415
	Slope	0.1922	0.5025
Humanistic Factors	Population density	0.1281	0.7157
	GDP	0.1506	0.6459

Additionally, the interaction analysis of driving factors (Figure 9) revealed that precipitation (X2) ∩ slope (X9) (q=0.9123) exhibited nonlinear enhancement. After the synergistic effect of the two factors, the explanatory power surged from 0.46 (single factor X2) to 0.91, strongly driving soil erosion synergistically. The combination of concentrated precipitation and steep slopes significantly enhanced runoff scouring force. Precipitation (X2) ∩ land use type (X1) (q=0.9015) also showed nonlinear enhancement, with a synergistic explanatory power close to 0.90. Bare land and farmland under heavy precipitation represent a "typical pattern" of high erosion risk: low vegetation coverage combined with concentrated runoff leads to a sharp increase in erosion risk. Precipitation (X2) ∩ vegetation coverage (X3) (q=0.4938) demonstrated dual-factor enhancement, with improved synergistic explanatory power (> single factor X2). The combination of low vegetation coverage and intense precipitation exacerbates erosion.

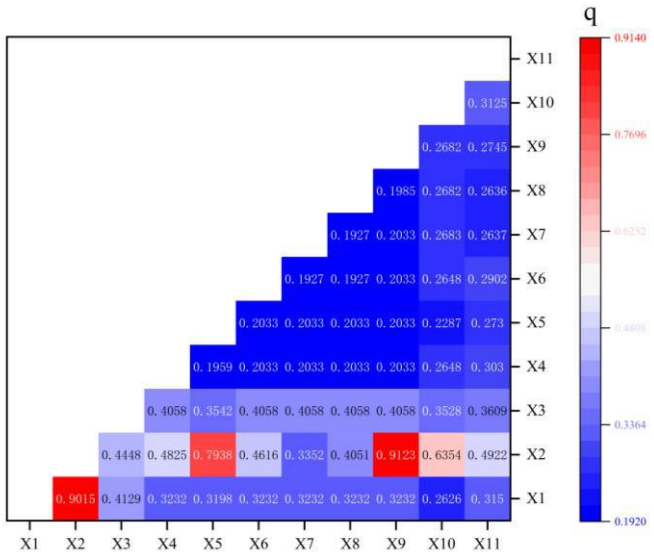

NOTE：X1：land use type X2：annual precipitation X3：vegetation coverage X4：soil organic carbon content X5：clay content X6：sand content X7：silt content X8：elevation X9：slope gradient ;X10：population density X11:GDP

Fig.9 Interaction Diagram of Driving Factors for Soil Erosion

4.5 Analysis of Spatiotemporal Distribution of Carbon Sequestration

4.5.1 Characteristics of Temporal Changes in Carbon Sequestration

According to the model calculations, the carbon sequestration in Zhanjiang City was 32.561 t/ha in 2013, 32.588 t/ha in 2018, 32.597 t/ha in 2020, and 32.652 t/ha in 2023, showing an overall upward trend. When analyzed by land use type (Figure 10), the carbon sequestration from largest to smallest is forest land > cropland > construction land > grassland > water bodies > unused land. By 2023, forest land accounted for 50.10% of the total carbon sequestration in Zhanjiang City, followed by cropland (38.33%) and construction land (2.411%). Overall, from 2013 to 2023, the soil erosion modulus decreased, and carbon sequestration capacity improved. Both grassland carbon sequestration and construction land carbon sequestration showed fluctuating increases, rising by 329.37 tons and 2,427.04 tons, respectively.

Using carbon sequestration dynamics from land use type conversions between 2020 and 2023, the relationship between soil erosion and carbon sequestration was explored. The conversion of cropland to forestland (an area of 6.00 km²) resulted in a net increase in carbon sequestration (104.28 t), with simultaneous accumulation in vegetation carbon (36.72 t) and soil carbon (67.56 t). This may be attributed to the restoration of forest vegetation, where increased vegetation cover intercepts rainfall and stabilizes soil, reducing hydraulic erosion's stripping of topsoil. Additionally, the input of vegetation litter enhances soil organic carbon, establishing a positive feedback loop of "erosion reduction-carbon sequestration." Conversely, the conversion of forestland to cropland (an area of 7.00 km²) led to a significant decrease in carbon sequestration (-121.66 t), with synchronous losses in vegetation carbon (-42.84 t) and soil carbon (-78.82 t) (Table 5). This is directly related to the decline in vegetation coverage after forestland reclamation. The destruction of forest ecosystems reduces soil erosion resistance (e.g., aggregate stability and root soil-binding capacity), making topsoil more susceptible to striping by rainfall and runoff. This results in the loss of organic-rich topsoil and weakens the ecosystem's carbon sequestration capacity, reflecting the logical chain of "vegetation destruction → intensified erosion → carbon loss."

In addition, the conversion of water bodies to grassland (covering an area of 1.00 km²) resulted in a significant increase in carbon sequestration (103.87t), with both vegetation carbon (97.91t) and soil carbon (5.96t) rising simultaneously (Table 5). When water bodies are transformed into grassland, the aquatic carbon pool is disrupted, but the development of grassland vegetation promotes the sedimentation of silt (carrying organic carbon). If hydraulic erosion occurs in the area, the silt eroded and transported from around the water bodies can accumulate during grassland restoration, serving as a potential source of soil carbon replenishment.

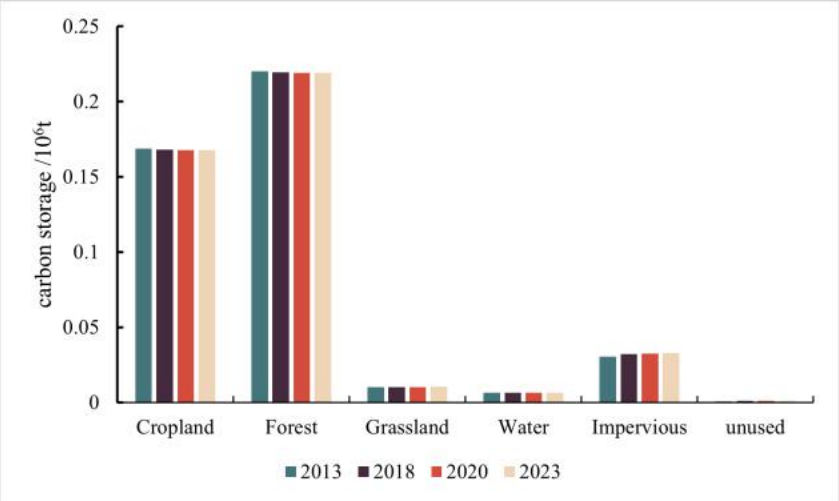

Fig.10 Carbon Sequestration by Land Use Type for Each Year

Table 5 Land Use Type Conversion and Corresponding Carbon Stock Changes from 2020 to 2023

Land use type change	Area/km²	Changes in carbon sequestration/t	Changes in vegetation carbon sequestration/t	Changes in soil carbon sequestration/t
Cropland-Cropland	5624.00	0.00	0.00	0.00
Cropland -Forestland	6.00	104.28	36.72	67.56
Cropland - Grassland	1.00	80.06	80.67	-0.61
Cropland - Water bodies	1.00	-23.81	-17.24	-6.57
Cropland - Construction	6.00	10.74	-32.04	42.78
Forestland - Cropland	7.00	-121.66	-42.84	-78.82
Forestland - Forestland	4640.00	0.00	0.00	0.00
Forestland - Grassland	1.00	62.68	74.55	-11.87
Forestland - Water bodies	1.00	-41.19	-23.36	-17.83
Forestland - Construction	4.00	-62.36	-45.84	-16.52
Water bodies - Forestland	1.00	-62.68	-74.55	11.87
Grassland - Grassland	93.00	0.00	0.00	0.00
Water bodies - Cropland	1.00	23.81	17.24	6.57
Water bodies - Grassland	1.00	103.87	97.91	5.96
Water bodies - Water bodies	1082.00	0.00	0.00	0.00
Water bodies - Construction	3.00	76.80	35.70	41.10

4.5.2 Spatial Variation Characteristics of Carbon Sequestration

In terms of spatial distribution, the carbon sequestration patterns in Zhanjiang City across different periods are relatively consistent, exhibiting an overall "higher in the north and lower in the south, with localized variations" characteristic (Figure 11). By comparing it with the spatial distribution map of land use types in Zhanjiang City (Figure 12), it can be observed that areas with high carbon sequestration per unit area are primarily located in forested and natural ecological regions in the northern and western parts of the city. Conversely, areas with low carbon sequestration per unit area are concentrated in water bodies and croplands with intensive human activities in the central, eastern, and surrounding regions. The increase in carbon sequestration is mainly attributed to ecological restoration and improved vegetation coverage, showing scattered distribution in localized areas. The decrease in carbon sequestration is largely associated with the expansion of construction land and intensified land development, primarily concentrated in urban core development zones and their peripheries. Overall, while the spatial distribution characteristics of the city's average carbon sequestration show minor localized adjustments over time, the general pattern remains closely linked to ecological changes and human activities.

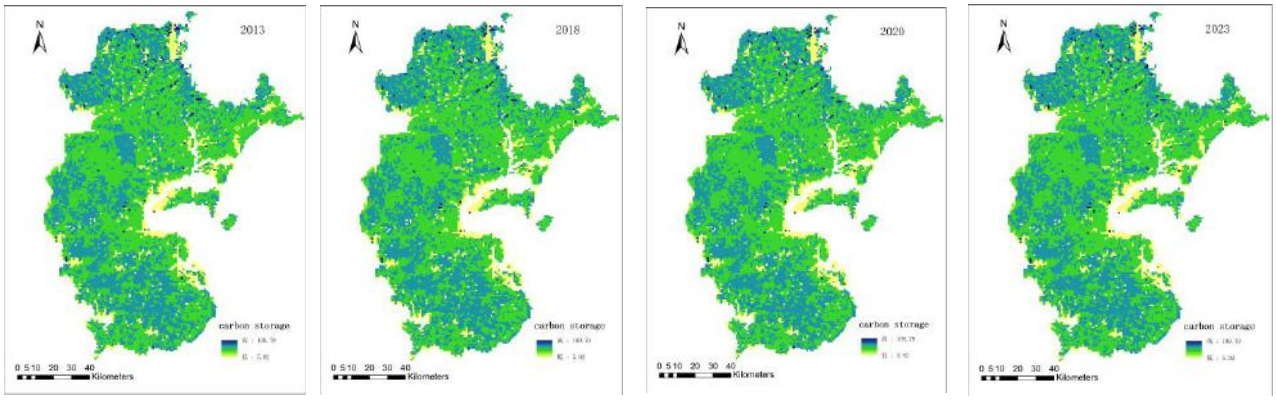

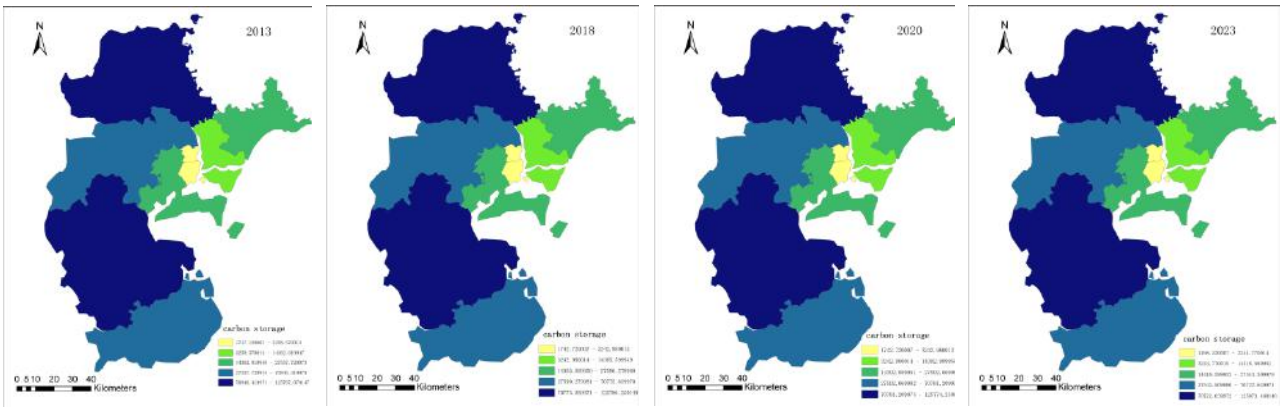

Fig.11 Spatial Distribution of Carbon Sequestration in Zhanjiang

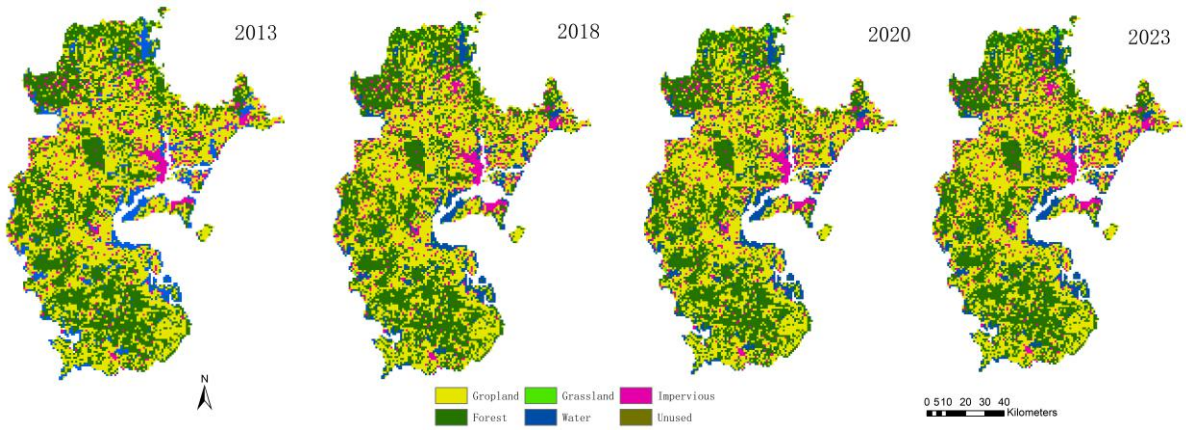

Fig.12 Spatial Distribution of Land Use Types in Zhanjiang City

V. CONCLUSION

(1) The intensity of soil erosion in Zhanjiang City exhibits spatial heterogeneity. Areas with moderate and moderate erosion are primarily distributed in the southern and eastern regions. The overall trend of soil erosion in Zhanjiang City is dominated by slight erosion, accounting for over 98.13% of the total eroded area. From 2013 to 2023, the area of slight erosion showed a trend of first decreasing and then increasing, with an average rate of 0.061 km²/year. The area of mild erosion displayed a similar trend of first decreasing and then increasing, with an average rate of -0.064 km²/year. The areas of moderate, strong, and extremely strong erosion all exhibited a trend of first decreasing and then increasing, with average rates of 0.053 km²/year, 0.033 km²/year, and 0.001 km²/year, respectively.

(2) From 2013 to 2023, the soil erosion intensity in Zhanjiang City generally showed a fluctuating trend. During the periods of 2013–2017, 2017–2020, and 2020–2023, 96.44%, 88.70%, and 99.16% of the areas, respectively, experienced no change in erosion intensity levels. The dynamic degree of slight erosion was predominantly negative in 2013–2017 and 2020–2023, indicating a gradual reduction in such areas, with more transitioning to mild erosion or higher levels. Meanwhile, the dynamic degrees of mild, moderate, strong, and extremely strong erosion were mainly positive, reflecting an ongoing increase in erosion area and worsening conditions. Notably, during 2020–2023, the dynamic degree of strong erosion peaked at 412.5%. Although most erosion intensities showed negative dynamic degrees from 2017 to 2020, suggesting some mitigation, the dynamic degrees of moderate and strong erosion surged again to 131.8%, 63.40%, and 412.5% in 2020–2023, indicating that the trend of intensifying erosion remains unchecked and urgent governance reinforcement

is needed.

(3) Based on the factor analysis of the geographic detector model, this study selected 11 factors for quantitative analysis with the soil erosion modulus in Zhanjiang City. The single-factor analysis revealed that among natural factors, annual precipitation and land use type are the primary factors influencing soil erosion, with annual precipitation exhibiting the strongest explanatory power. In 2020, the precipitation erosivity factor significantly decreased, corresponding to a notable decline in the soil erosion modulus for the same year, highlighting the dominant role of precipitation. Among human activity factors, GDP demonstrated relatively high explanatory power. The interaction factor analysis results indicated that all interactions between factors exhibited either two-factor enhancement or nonlinear enhancement characteristics. When the factors influencing soil erosion changes interacted, their synergistic driving effects were significantly stronger than those of individual factors. Interactions such as precipitation ∩ slope and precipitation ∩ land use notably enhanced the explanatory power for the spatial differentiation of the erosion modulus.

(4) The conversion of land use profoundly influences the carbon sequestration "source-sink" process by altering vegetation cover, soil erosion resistance, and erosion environment. The "carbon accumulation" from cropland to forestland and the "carbon loss" from forestland to cropland are essentially the result of the combined effects of soil erosion risk and changes in vegetation ecological functions. This provides a typical scenario for quantifying the "erosion-carbon sequestration" relationship and also offers a basis for optimizing regional carbon sequestration and soil erosion processes through land use regulations.

(5) From 2020 to 2023, as the dominant influencing factor of soil erosion in Zhanjiang City (precipitation factor) intensified, coupled with changes in land use types (conversion of forest land to cropland), the intensity of soil erosion increased. The enhanced erosion stripped away the topsoil rich in organic matter, exposing previously stable carbon to an oxidizing environment and accelerating its decomposition (CO_2 release). Consequently, carbon sequestration declined, the climate regulation function weakened, and the performance of the ecological service system was affected.

(6) Based on the above analysis, in order to effectively manage and protect the soil resources in this region, this study proposes strengthening the management and monitoring of areas with complex terrain, implementing soil and water conservation measures such as vegetation restoration, gully control, and shelterbelt construction to reduce the risks of soil erosion and water resource loss. Additionally, continuous monitoring of soil erosion conditions and timely adjustment of management strategies are crucial for restoring the ecological balance of the area and achieving sustainable development.

ACKNOWLEDGEMENTS

The author is grateful for the research grants given to Ruei-Yuan Wang from GDUPT Talents Recruitment (No.2019rc098), Peoples R China under Grant No.702-519208, and Academic Affairs in GDUPT for Goal Problem-Oriented Teaching Innovation and Practice Project Grant No.701-234660.

REFERENCES

[1] Babbar, D., Areendran, G., Sahana, M., Sarma, K., Raj, K., and Sivadas, A. Assessment and prediction of carbon sequestration using Markov chain and InVEST model in Sariska Tiger Reserve，India. Journal of Cleaner Production， 2021，278：123333.

[2] Chen, J. X., Yue, D. P., Wang, J. P., et al. Development and Application of GIS - based Calculation System for Soil Erosion. Journal of Northwest Forestry University, 2016, 31(01): 206 - 213.

[3] Chen, Z. F. Study on Soil Loss Equation in Chongqing Based on RUSLE Model. Chongqing: Southwest University, 2011.

[4] Dai, Y. F., Li, H. X., and Tang, Y. H. Spatiotemporal Evolution and Driving Force Analysis of Carbon Storage in Terrestrial Ecosystems of Guangdong Province. Journal of Foshan University (Natural Science Edition), 2025, 43(04): 29-36. DOI: 10.13797/j.cnki.jfosu.1008-0171.2025.0048.

[5] Deng, C., Liu, J., Liu, Y., Li, Z., Nie, X., Hu, X., Wang, L., Zhang, Y., Zhang, G., Zhu, D., and Xiao, L. Spatiotemporal dislocation of urbanization and ecological construction increased the ecosystem service supply and demand imbalance. Journal of Environmental Management，

2021，288：112478.

[6] Dotterweich, M. The history of human-induced soil erosion: Geomorphic legacies, early descriptions and research, and the development of soil conservation—A global synopsis. Catena, 2013, 201: 1-34.

[7] He, Y., Chen, Y. C., TALAT Ahmed Ehab, et al. Spatiotemporal Characteristics and Trend Prediction of Soil Erosion in the Kuye River Basin. Journal of Soil and Water Conservation, 2024, 38(05): 10 - 19. DOI: 10.13870/j.cnki.stbcxb.2024.05.028.

[8] Hu, X., Zeng, C., Qian, Q.H., Wang, Q., and Li, Y. B. Using RUSLE Model to Analyze Temporal and Spatial Characteristics of Soil Erosion in Tongren Area From 1987 to 2015. Journal of Ecology and Rural Environment, 2019, 35(2): 158-166.

[9] Huang, Q. L., Shi, C. Q., Zhao, T. N., et al. Study on Soil Erosion in Xing'an League Region from 1985 to 2023 Based on RUSLE Model and Optimal Geodetector. Research of Soil and Water Conservation, 2025, 32(06): 1 - 10 + 20. DOI: 10.13869/j.cnki.rswc.2025.06.031.

[10] Jin, C. X. Temporal and Spatial Distribution Characteristics of Rainfall Erosivity in Henan Province from 1986 to 2015. Henan Water Resources and South-to-North Water Diversion, 2019, 48(10): 63-65.

[11] Li, Y., Li, Q., and Zang, Q. Spatial-temporal Characteristics Analysis of Soil Erosion in Karst Watershed Based on GIS Technology and RUSLE Model——A Case Study of Wujiang River Basin in Guizhou Province. Hydropower and Pumped Storage, 2023,01:69-74.

[12] Liang, J. F., Wei, X. C., Ma, L. S., et al. Study on Soil Erosion in Sansui County, Guizhou Province Based on RUSLE Model. Pearl River, 2019, 40(8): 13-18, 31.

[13] Liu Y., Zhang, J., Zhou, D. M., Ma, J., Dang, R., Ma, J. J., and Zhu, X. Y. Temporal and spatial variation of carbon storage in the Shule River Basin based on InVEST model. Acta Ecologica Sinica, 2021, 41(10): 4052-4065.

[14] Liu, X. H. Analysis and Extraction of Topographic Factors for Regional Soil and Water Loss. Yangling: Northwest A&F University, 2001: 1-53.

[15] Ma, S., Qiao, Y. P., Wang, L. J, and Zhang, J. C. Terrain gradient variations in ecosystem services of different vegetation types in mountainous regions：Vegetation resource conservation and sustainable development. Forest Ecology and Management，2021，482：118856. doi:10.1016/j.foreco.2020.118856

[16] McCool, D. K., Brown, L. C., Foster, G. R., et al. Revised Slope Steepness Factor for the Universal Soil Loss Equation. Transactions of the ASABE, 1987, 30(5): 1387-1396.

[17] Nelson, E., Mendoza, G., Regetz, J., Polasky, S., Tallis, H., Cameron, D., Chan, K.M., Daily, G.C., Goldstein, J., Kareiva, P. M., and Environment, t. Modeling multiple ecosystem services, biodiversity conservation, commodity production, and tradeoffs at landscape scales. Front. Ecol. Environ. 2009, 7 (1), 4–11. https://doi.org/10.1890/ 08002

[18] Qi, S. H., Jiang, M. X., and Yu, X. B. Assessment of Soil Erosion in Jiangxi Province from 1995 to 2005 Based on Remote Sensing and ULSE Model. China Environmental Science, 2011, 31(7): 1197-1203.

[19] Sharply, A. N., and Williams, J. R. EPIC Erosion/Productivity Impact Calculator: 1. Model Documentation. Technical Bulletin - United States Department of Agriculture, 1990, 1768: 235.

[20] Wang, B. Z., Bi, R. T., Chen, L. G., et al. Spatial Characteristics of Soil Erosion in the Loess Area of the Upper Hutuo River Based on USLE Model. Chinese Agricultural Science Bulletin, 2020, 36(7): 76-82.

[21] Wang, C. J., Tang, X. H., and Zheng, D. X. Evaluation of Soil Erosion Sensitivity Supported by GIS. Bulletin of Soil and Water Conservation, 2005, 25(1): 68-74.

[22] Wang, T. Remote Sensing Monitoring of Soil Erosion in the Three Gorges Reservoir Area and Its Scale Effect. Wuhan: Huazhong Agricultural University, 2011.

[23] Williams, J. R., Renard, K. G., and Dyke, P. T. EPIC: A New Method for Assessing Erosion's Effect on Soil Productivity. Journal of Soil and Water Conservation, 1983, 5: 381-383.

[24] Wu C., Lü H., Zhou Z., Xiao W., Wang P., and Wang T. Spatial distribution analysis of soil erosion in the Three Gorges Reservoir Area. Science of Soil and Water Conservation, 2012, 10(3): 15-21.

[25] Wu, J. and Wang, R.Y. Study on Soil Erosion Characteristics in Maoming Based on USLE and InVEST Models. Global Journal of Arts Humanity and Social Sciences, 2023, 3(5): 534-542.

[26] Yan, X. P. Study on the Characteristics of Soil Erosion in Chengde City Based on RUSLE Model. Sichuan Agricultural University, 2022. DOI:

10.27345/d.cnki.gsnyu.2022.001243.

[27] Yang, C. J., Liu, J. Y., and Zhang, Z. X. Spatial Analysis of Soil Erosion and Its Background in Chongqing. Journal of Soil and Water Conservation, 2000, (03): 84 - 87.

[28] Zhang, K. L., Peng, W. Y., and Yang, H. L. Erodibility Value of Soils in China and Its Estimation. Acta Pedologica Sinica, 2007, (1): 7-13.

[29] Zheng, Q. Y., Zhao, G. Y., Yang, P., et al. Study on Soil Erosion in the Black Soil Region of Northeast China Based on RUSLE Model. Rural Science & Technology, 2023, 14(18): 145-148. DOI: 10.19345/j.cnki.1674-7909.2023.18.026.

[30] Zhou, J. Analysis of Ecosystem Service Assessment and Driving Factors in Dongting Lake Basin Based on InVEST Model. Central South University of Forestry and Technology, 2025. DOI: 10.27662/d.cnki.gznlc.2025.000230.

[31] Zuo, L. L., Liu, G. H., Zhao, J. Y., Li, J. J., Zheng, S. Y., Wang, J. C., and Su, X. K. Effects of ecosystem services on sustainable development goals in western Sichuan. Acta Ecologica Sinica, 2024, 44(10): 4203-4216.